Mixed Surfactant Based Microemulsions as Vehicles for Enhanced Solubilization and Synthesis of Organoselenium Compounds

S. K. Mehta,* Khushwinder Kaur, Ekta Arora, and K. K. Bhasin

Department of Chemistry and Centre of Advanced Studies in Chemistry, Panjab University, Chandigarh, 160 014 India

Received: March 28, 2009; Revised Manuscript Received: May 27, 2009

We exploited the added degree of compositional freedom provided by mixed AOT/lecithin surfactants in reverse isooctane microemulsion to demonstrate that a small amount of added lecithin significantly enhances the solubility of organodiselenides over that in AOT reverse isooctane microemulsions alone. Conductivity results show that the added lecithin significantly increases the solubility of four different organodiselenides and raises the temperature required to induce percolation. FTIR, ^{1}H NMR, and UV−visible techniques were utilized to gain insight into the interactions of organodiselenides, AOT and lecithin headgroups with water in the micellar core. The information obtained from these experiments was used to design a novel synthetic route for preparing 4-chloro-2-(naphthalen-2-ylselanyl) pyrimidine in reverse microemulsion.

Introduction

Microemulsions are stable, transparent solutions of water, oil, and surfactant and have been described as consisting of spherical droplets of disperse phase separated from a continuous phase by a surfactant film.[1−3] The surfactant aggregates in microemulsions are closely packed globules where the polar headgroup of the surfactant molecule occupies the interior of the aggregates and the hydrophobic tail extends in the bulk apolar solvent with water encapsulated in compartments.[3−7] Microemulsions as chemical reaction media are interesting subjects of study because these media are macroscopically homogeneous, isotropic, and heterogeneous on a microscopic scale.[8] Their structural characteristics offer the opportunity to solubilize and stabilize relatively large and otherwise insoluble molecules in the microemulsion core. The physiochemical properties of such systems are often very different from those of unsolvated molecules or condensed phases being more or less influenced by confinement effects, inhomogeneous distribution, orientation order, and interfacial interactions.[9,10] In recent years, various research groups have shown an increased interest in the assimilation of additives in the microemulsion media.[11−14]

The structure of the surfactant also plays a dramatic role in the properties of microemulsions and the amount of additive hosted by them. The anionic surfactant bis(2-ethylhexyl)sodium sulfosuccinate (AOT) has a surfactant packing parameter, *P*, of 1.1 and tends to have a spontaneous curvature that is concave toward water.[15] The macroscopically single phase water-in-oil microemulsions of AOT can incorporate water typically to water/AOT (ω = [water]/[AOT]) level of 30−40 and sufficient quantities of the additive. The zwitterionic surfactant phosphatidylcholine, i.e., lecithin (LC), has a significantly larger headgroup but a smaller packing parameter of 0.6 compared to AOT.[15−17] In aqueous systems, LC tends to form interfaces with minimal curvature. The combination of AOT and LC further leads to a highly rigid gel that can incorporate a significantly high amount of water (ω = 50−70).[18,19]

Our interest lies in the microemulsion formed by the mixing of AOT and LC in water and isooctane leading to ME-I (water/AOT/isooctane) and ME-II (water/AOT+LC/isooctane) microemulsions and assimilation of organodiselenides viz., dipyrimidyl derivatives such as, bis(4-dimethylamino-2-pyrimidyl) diselenide ($C_{12}N_6H_{16}Se_2$), bis(4-chloro-2-pyrimidyl) diselenide ($C_8N_4H_4Se_2Cl_2$), dinapthyl diselenide, (Nap_2Se_2) and bis(diphenyl methyl) diselenide $(Ph_2CHSe)_2$ in ME-I and ME-II. In addition, the synthesis of 4-chloro-2-(naphthalen-2-ylselanyl) pyrimidine in microemulsion media employing 2,4-dichloropyrimidine as starting reagent has also been attempted.

Organodiselenides are relatively large molecules and are insoluble in aqueous media. The compound $(Ph_2CHSe)_2$ is considered to be a derivative of methyl selenide that lacks the repulsive smell but possesses a good shelf life with interesting chemical behavior. Pyrimidyl, napthyl and phenyl derivatives have been taken into account to make comparative studies between the behaviors of aromatic selenium compounds in microemulsion media. The napthyl moiety consists of fused, planar, and rigid aromatic ring systems with 10π electrons that result in remarkable differences in its properties as compared to the phenyl[20] and pyrimidyl analogues. The pyrimidyl moiety is found in natural products and widely used as inhibitors of human immunodeficiency virus, as effective anticancer drugs,[22,23] besides being antirejection drugs in transplantations.

Water-in-oil microemulsions exhibit a low electrical conductivity as the layers of surfactant separate water droplets. However, when the temperature, θ, increases beyond the critical value (i.e., θ_c), the conductivity increases sharply. This sudden rise in conductance has been related to an increase in the attractive interactions between the droplets that facilitate migration of surfactant counterions along connected paths through the microemulsion, leading to the phenomenon of electric percolation.[11−14]

To date, no data has been reported on the synthesis of organoselenides in microemulsion media (to the best of our knowledge). However, there exists extensive evidence of the ability of microemulsions to influence reaction rates and equilibria, e.g., the hydrolysis of hydroxamic acids[25−27] and other carboxylic acid derivatives.[28] Interesting reports exist in literature

* To whom correspondence should be addressed. E-mail: skmehta@pu.ac.in. Tel: +91-172-2534423. Fax: +91-172-2545074.

10.1021/jp902801g CCC: $40.75
Published on Web 07/09/2009

SCHEME 1: Structures of (A) AOT (B) and Lecithin

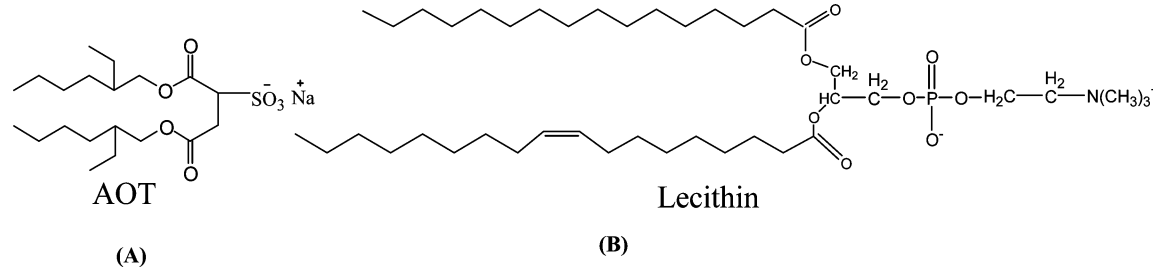

SCHEME 2: Schematic Structure Representations of Organodiselenides (I) $C_{12}N_6H_{16}Se_2$, (II) $C_8N_4H_4Se_2Cl_2$, (III) Nap_2Se_2, and (IV) $(Ph_2CHSe)_2$

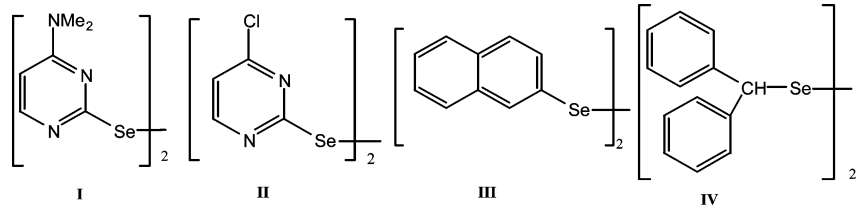

on the kinetics of chemical reactions on microemulsions.[28,29] Prediction and/or interpretation of the kinetic influence of these media are relatively easy when the reagents congregate in the aqueous micro droplets that act as variable size nanoreactors concentrating the reagents.[30]

Experimental Section

Materials. Sodium bis(2-ethylhexyl) sulfosuccinate (AOT; Fluka, purity >99%), lecithin (LC) extracted from soybeans, (Fluka, purity >95%), isooctane (E-Merck, purity >99%), $NaBH_4$ (Fluka, purity >98%), ethanol (Fluka, purity >99%), and DMF (Fluka, purity >99%) were used as received. Organodiselenides including $(Nap_2Se_2$, $(Ph_2CHSe)_2$, $C_{12}N_6H_{16}Se_2$, $C_8N_4H_4Se_2Cl_2)$, and $C_4N_2H_2Cl_2$ were synthesized in the laboratory and characterized through various spectroscopic techniques.[20] The structures of AOT, lecithin, and assimilated organodiselenides have been presented in Schemes 1 and 2. Triple distilled water with conductance less than 3 μS cm^{-1} was used for the preparation of MEs.

Conductivity Measurements. Electrical conductivity measurements of the samples were carried out with Pico digital conductivity meter operating at 50 Hz from Labindia instruments with an absolute accuracy of ±3% and precision of ±0.1%. The cell constant used was 1.0 cm^{-1}. The temperature was kept constant with the help of RE320 Ecoline thermostat with an accuracy of ±0.01K.

FTIR Spectroscopy. FTIR spectra were recorded in the spectral region of 4400−350 cm^{-1} using Perkin-Elmer (RX1) FTIR spectrophotometer with AgCl windows.

UV−Vis Absorption Spectroscopy. UV−vis absorption spectra were obtained in the spectral range of 250−500 cm^{-1} using Jasco 530 spectrophotometer with precision of ±0.2 nm using quartz cells with a path length of 1 cm^{-1}.

NMR Spectroscopy. ^1H chemical shifts were observed with the help of Bruker AC 400 NMR. Spectral calibration was performed using D_2O or CCl_4-CDCl_3 as internal standard. ^{13}C and ^{77}Se chemical shifts were observed with the help of Jeol 300 NMR.

Mass Spectrometry. The mass spectrum was obtained on a Q-TOF micromass spectrometer.

Preparation of Samples. A series of experiments were carried out and [AOT] = 0.784 M and [AOT]:[LC] = 0.774M:0.01 M at $\omega = 30$ were found to be most acceptable concentrations to enhance assimilation of organodiselenides. All the samples were transparent and optically clear. For the synthesis of 4-chloro-2-(naphthalen-2-ylselanyl) pyrimidine ($C_{14}N_2H_9SeCl$), wide range of ME compositions $\omega = 2$ to 40 have been used in case of both ME-I (water/AOT/isooctane) and ME-II (water/AOT + LC/isooctane). This allowed us to modify the droplet size (by changing ω) and the maximum 2,4-dichloropyrimidine ($C_4N_2H_2Cl_2$) intake capacity. Variable surfactant concentrations have been tried up to a total surfactant concentration of 0.784 M. However, ME formulated at $\omega = 30$ and [AOT:LC] = 0.784 M was found to be the most suitable to work with. The tried lower surfactant concentrations could not assimilate significant quantity of compound for the reaction to take place. ME-I could not be used for synthesis due to similar reasons. Moreover, it did not support 3.5 mL of C_2H_5OH-DMF, and the solution turned turbid. Therefore, ME-II was used to carry out the synthesis of $C_{14}N_2H_9SeCl$.

Results and Discussion

Although the basic understanding of the percolation phenomenon in AOT based microemulsion[11−14] has been fairly studied, however, the knowledge of percolation[31] in AOT/LC mixed microemulsion is limited. Hong et al.[31] have reported that the addition of small amounts of LC to AOT based microemulsions stabilized the micellar interface and the leakage of encapsulated β-galactosidase to the bulk aqueous phase was therefore negligible. They have also tried to relate specific interfacial properties, which affect protein extraction in AOT and AOT/LC microemulsions with percolation processes. The comparative percolation study of AOT and lecithin microemulsions has also been carried out by Fontanella et al.[32] Percolation phenomenon in branched lecithin microemulsions has also been reported by Aliotta and Fazio.[33] The current percolation study has been undertaken with a view that percolation phenomenon is a sensitive and convenient measure of microinterface of microemulsions[31] solubilizing various organodiselenides which clearly reflects the chalogen-micellar and micellar-micellar interactions. This provides a better insight into the specific interfacial properties, which affect organodiselenide solubilization and behavior in the AOT and AOT−lecithin microemul-

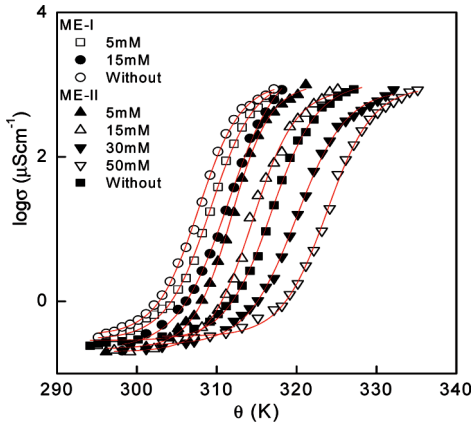

Figure 1. Variation of temperature of $C_{12}N_6H_{16}Se_2$ for ME-I and ME -II at [AOT:LC] = [0.774:0.01] (solid red lines show SBE fitting).

TABLE 1: Percolation Threshold Temperature for ME-I at Different Organodiselenide Concentrations[a]

organodiselenide	[conc.] (mM)	log σ_i	log σ_f	θ_c (K) differential	θ_c (K) SBE
		ME-I			
without		-0.46 ± 0.02	3.02 ± 0.03	308.55	307.73
$C_{12}N_6H_{16}Se_2$	5	-0.59 ± 0.02	3.30 ± 0.06	309.55	309.68
	15	-0.66 ± 0.02	3.39 ± 0.09	313.64	313.64
$C_8N_4H_4Se_2Cl_2$	5	-0.52 ± 0.02	3.09 ± 0.05	311.11	309.22
Nap_2Se_2	5	-0.52 ± 0.02	3.09 ± 0.05	311.05	309.22
	15	-0.66 ± 0.03	3.39 ± 0.09	312.05	311.44
$(Ph_2CHSe)_2$	5	-0.63 ± 0.01	2.94 ± 0.01	310.00	310.46
		ME-II			
without		-0.54 ± 0.01	3.02 ± 0.03	312.05	316.87
$C_{12}N_6H_{16}Se_2$	2.5	-0.61 ± 0.01	2.88 ± 0.03	318.13	317.88
	5	-0.60 ± 0.02	2.82 ± 0.03	318.63	318.56
	15	-0.60 ± 0.02	2.93 ± 0.02	319.15	319.99
	50	-0.57 ± 0.01	3.43 ± 0.05	327.15	326.17
$C_8N_4H_4Se_2Cl_2$	5	-0.47 ± 0.02	3.04 ± 0.05	319.15	318.23
	15	-0.48 ± 0.04	3.17 ± 0.01	320.15	320.55
	20	-0.48 ± 0.02	2.96 ± 0.03	323.10	321.80
Nap_2Se_2	5	-0.65 ± 0.02	3.01 ± 0.03	313.05	311.85
	15	-0.69 ± 0.02	2.94 ± 0.04	314.05	314.49
	30	-0.60 ± 0.02	2.93 ± 0.02	319.05	319.99
	50	-0.48 ± 0.03	2.96 ± 0.03	324.07	323.80
$(Ph_2CHSe)_2$	2.5	-0.61 ± 0.01	2.88 ± 0.03	318.63	317.88
	5	-0.60 ± 0.02	2.93 ± 0.02	319.15	319.99
	15	-0.48 ± 0.02	3.17 ± 0.01	320.15	320.65

[a] log σ_i = initial conductance, log σ_f = final conductance.

sions. The solubilization behavior obtained thus opens the gateway for organic synthesis.

Dependence of Conductivity on Temperature. Temperature is known to have great influence on the properties and dynamics of MEs.[11−14] The conductance behavior of ME-I and ME-II has been monitored when the temperature was varied under a constant composition. The solubilization increases from 2.5 to 50, 20, 50, and 15 mM for $C_{12}N_6H_{16}Se_2$, $C_8N_4H_4Se_2Cl_2$, Nap_2Se_2, and $(Ph_2CHSe)_2$ in ME-II as compared to 15, 5, 15, and 5 mM in ME-I. The temperature-conductance profiles of $C_{12}N_6Se_2H_{16}$ at different concentrations viz., 2.5, 5, 15, and 30 mM for ME-I and 2.5, 5, 15, and 30 mM for ME-II have been depicted in Figure 1. The percolation parameters for ME-I and ME-II have been tabulated in Table 1. The plots have been fitted to SBE[34]

$$\log \sigma = \log \sigma_f \left[1 + \left(\frac{\log \sigma_i - \log \sigma_f}{\log \sigma_f}\right) \times \{1 + \exp(\theta - \theta_c)/\Delta\theta\}^{-1}\right] \quad (1)$$

where σ and θ represent conductance and temperature, $\Delta\theta$ is the constant interval of θ and i, f, and c stand for initial, final, and percolation stages respectively. At constant composition, organodiselenides have been found to delay the percolation process. The delay becomes more pronounced with the increase in concentration of organodiselenide. The value of θ_c for compositions under study varies as $C_8N_4H_4Se_2Cl_2 \sim Nap_2Se_2 > (Ph_2CHSe)_2 > C_{12}N_6H_{16}Se_2 >$ without for ME-I and $C_8N_4H_4Se_2Cl_2 > (Ph_2CHSe)_2 \sim C_{12}N_6H_{16}Se_2 > Nap_2Se_2 >$ without for ME-II at [organodiselenide] = 5 mM.

Maitra et al.[35] have reported that in the percolative ME the droplets retain their closed structure although infinite clusters are formed due to inter droplet interactions. The mutual contact and the bridging between the droplets is due to the presence of additives either at the interface (e.g., hydrotopes and bile salts)[11] or in the core of the droplets (e.g., poly (ethylene glycol)s).[13] The pyrimidyl derivatives have two active N-ends that anchor the droplet surface. This results in the bridging of the nanodroplets and the conduit formation is favored. The pyrimidyl derivative is a rigid nonplanar moiety in which one (pyrimidyl−Se−)− unit is bent leaving the central horizontal plane. It contains electronically active −(−Se−Se−)− along with two N-ends. The molecule adheres to the droplet interface resulting in bridging of the nanodroplets. The phenyl and napthyl derivatives of selenium have no such active sites except for −(−Se−Se−)− and remain in the dispersion medium, resisting the droplet fusion by enhancing the blockening effect and thus delaying the percolation threshold. However, in ME-II even the phenyl and napthyl derivatives may be restricted to the interface because the introduction of LC in ME-II leads to the immobilization of hydrophobic and hydrophilic regions which allows the formation of extended structures that are organized over multiple length scale.[18,36]

Surfactant molecules solubilized in MEs display a large variety of microstructures, which are sensitive to some control parameters such as temperature, size of water pool, effect of external entity, etc. The local geometric constraints and the subtle balance of opposing forces originating from polar head groups, and the hydrophobic tail of the surfactant molecules determine the morphology of self-assembling system. The calculation of thermodynamic parameters of ME-I and ME-II further indicates that the microenvironment of the system without organodiselenide is less organized as compared to the presence of organodiselenides. The higher value of θ observed in ME-II as compared to ME-I indicates the more organized surroundings of ME-II as compared to ME-I (Supporting Information).

The interactions between the organodiselenide and the MEs are best revealed by ^{1}H NMR, FT IR, and UV−vis absorption spectroscopy. The water pool properties of microemulsion have been extensively studied by FT IR and ^{1}H NMR.[37−40] Typical ^{1}H NMR spectra of ME-I and ME-II with and without organodiselenide reveal a unique peak due to aromatic region in organodiselenide molecules. Table 1 (Supporting Information) shows the comparison of peaks in ME-I and ME-II. The inspection of data reveals that the peaks due to aromatic protons are retained in ME-I and ME-II indicating that the organodiselenide moiety is intact in the ME system and is not subjected to any breakdown. Peaks due to aromatic protons and headgroup protons are downfield in ME-I as compared to ME-II. These findings are consistent with the fact that addition of LC in ME-I involves progressive change in the electron cloud of the protons of the headgroup. The organodiselenide interaction is mainly localized in the proximity of the polar head groups of the

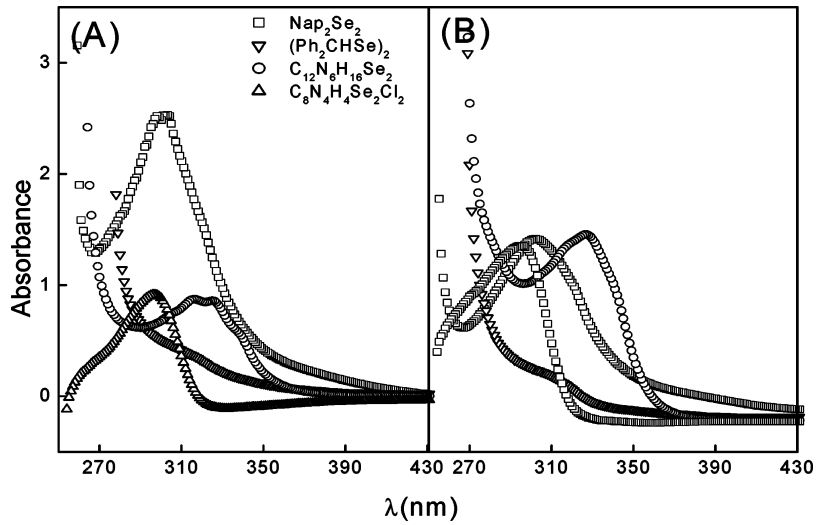

Figure 2. Variation of absorbance vs wavelength for organodiselenides (A) ME-I and (B) ME-II.

TABLE 2: Component Parameters Position Obtained from FT IR Stretching Bands of ME-I and ME-II at $\omega = 30$ in the Presence Organodiselenides

organodiselenide	OH (cm^{-1})	CO (cm^{-1})	SO_3^- (cm^{-1})	COC (cm^{-1})
without	3323.0,3343.1	1706.4,1704.5	1045.2,1046.1	1225.5,1225.1
$C_{12}N_6H_{16}Se_2$	3325.0,3336.3	1702.8,1707.3	1045.5,1045.8	1230.9,1225.3
$C_8N_4H_4Se_2Cl_2$	3325.4,3350.2	1702.9,1707.2	1045.6,1046.2	1225.5,1225.8
Nap_2Se_2	3326.6,3355.1	1702.8,1706.2	1046.0,1046.5	1225.6,1228.1
$(Ph_2CHSe)_2$	3325.0,3343.0	1702.8,1706.2	1044.2,1046.1	1225.6,1228.1

surfactant. This is revealed by the shifts of the headgroup protons in ME-I and ME-II.

The UV−vis absorption spectra of ME-I and ME-II have been recorded at different concentrations of organodiselenides. The organodiselenide bands have been presented in Figure 2, panels A and B, respectively. The observed trends in position and intensity of absorption bands depend upon the nature of electronic transition responsible for absorption and can be explained in terms of molecular orbital theory. The spectra of organodiselenide depend mainly on the three effects: inductive, hyperconjugative and torsional (steric).[41] The λ_{max} of organodiselenides in ME-I and ME-II falls within the range 284−320 nm. The λ_{max} for ME-I follows the order $C_{12}N_6H_{16}Se_2$ > $(Ph_2CHSe)_2$ > Nap_2Se_2 > $C_8N_4H_4Se_2Cl_2$ with peaks at 326.61, 315.95, 300.74, and 297.14 nm, respectively. Similar, trends have been observed in ME-II with peaks at 321.30, 309.6, 301.36, and 294.48 nm. The spectra did not show a sharp peak for $(Ph_2CHSe)_2$; only a broad band is observed. The observed band is due to the Se−$C_{10}H_7$ chromophore, which involves 4p electrons of Se in conjugation with 10π electrons of the napthyl ring. This is supported by the interpretation of UV−vis spectra of related compounds cited in literature.[42] The band at 300 nm in diselenide can be assigned to Se−Se chromophore.[43] The shifts observed in the spectra are an indication of the bonding strength of the added organodiselenide in the microemulsion. The greater ionic interactions observed among the (AOT+LC) moieties at the interface and the organodiselenide moiety can be held responsible for the blue shifts observed in ME-II as compared to ME-I. This is in line with the inference obtained from conductivity measurement which states that organodiselenides are more tightly held at the ME-II interface as compared to ME-I.

The stretching frequency in FT IR reflects the interaction between the surfactant molecules and the organodiselenides. Table 2 depicts the stretching frequencies of various bands in ME-I and ME-II. The state of organodiselenide in ME-I and ME-II can be rationalized in terms of organodiselenide entrapped in the interfacial layer of appropriately oriented AOT/AOT+LC monolayers. A comparison of OH band frequencies of the organodiselenides reveals a shift toward higher frequency of around 11.3, 24.8, 28.5, 18, and 20.1 cm^{-1}, respectively, for $C_{12}N_6H_{16}Se_2$, $C_8N_4H_4Se_2Cl_2$, Nap_2Se_2, $(Ph_2CHSe)_2$, and without in ME-II than ME-I. The peak centered at 1706 cm^{-1}, assigned to CO stretching shows a similar trend of shift towards the higher frequency with the incorporation of organodiselenide.

The high frequency values observed in ME-II as compared to ME-I further reveal the entrapping of organodiselenide at the interface. However, a shift of around 1 cm^{-1} observed for C−O−C and SO_3^- is modest. A representative spectrum for different absorption regions has been presented in Figure 3.

Preparation and Characterization of 4-Chloro-2-(naphthalen-2-ylselanyl) Pyrimidine $C_{14}N_2H_9SeCl$. To a solution of Nap_2Se_2 (0.53 mM, 0.022 g) in 3.5 mL of C_2H_5OH-DMF (6:1) was added 0.022 g of $NaBH_4$ in parts with continuous stirring at 0−5 °C, and the reaction was maintained under inert atmosphere of nitrogen so as to prevent oxidation of selenide anion. After 5 min of stirring, 152 mM (wrt ME) of $C_4N_2H_2Cl_2$ in ME-II with [AOT:LC] = 0.774M:0.01M, $\omega = 30$ was added dropwise. Completion of the reaction as evidenced by TLC was observed within 30 min. The obtained product was subjected to column chromatography using ethyl acetate as eluant, which gave the desired compound in 45% yield. $C_{14}N_2H_9SeCl$ was characterized using various spectroscopic techniques. ν_{max}/cm^{-1} 1541.5 and 1399.1(C=C), 791.0(C−Se) and 665.4(C−Cl); δ(ppm)^{1}H(400 MHz; $CDCl_3/CCl_4$; Me_4Si) 8.39−8.35 (1H, d, J 8.1, 5-H), 8.16−8.12 (2H, m, 8-H, 16-H), 8.04−7.98 (2H, m, 9-H,14-H), 7.63−7.59 (3H, m, 11-H, 12-H, 13-H), 6.52−6.50 (1H, d, J 5.2, 6-H); δ(ppm)^{13}C(75 MHz; $CDCl_3/CCl_4$; Me_4Si) 175.09, 160.63, 157.24, 137.41, 134.56, 134.45, 131.88, 128.97, 128.11, 127.67, 126.25, 124.29, 118.73. δ(ppm)^{77}Se(57 MHz;

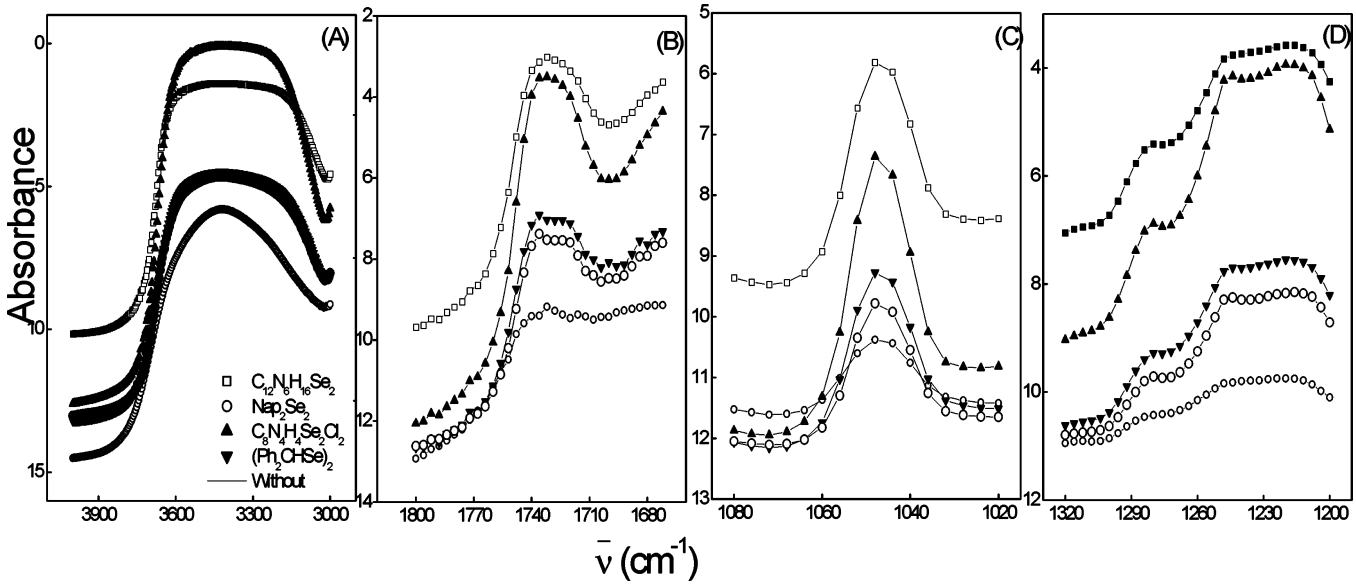

Figure 3. Comparison of infrared stretching band of ME-II at $\omega = 30$ in the presence of 10 mM organodiselenide showing different stretching regions (A) OH, (B) CO, (C) SO_3^-, and (D) COC ester linkage.

$CDCl_3/CCl_4$; Me_2Se) 427.57; *m/z* 323, 9% ($[C_{14}N_2H_9SeCl]^{+\bullet}$ + 3) and 285, 30% ($[C_{14}N_2H_9Se]^{+\bullet}$).

Proposed Mechanism for Synthesis of (4-Chloro-2-(naphthalen-2-ylselanyl) Pyrimidine ($C_{14}N_2H_9SeCl$). Our interest in the synthesis of $C_{14}N_2H_9SeCl$ originated from the fact that general synthetic procedures[44−49] employed for the synthesis of organochalcogen compounds are rather complicated as they involve long refluxing, controlled experimental conditions, and high cost. The Bhasin group[50] has synthesized 4-chloro-2-(naphthalen-2-ylselanyl) by a conventional method using sodium borohydride as the reducing agent. The reaction completes in 3 h but involves work up with costly solvents. Therefore, development of a practical, efficient, and quick process is quite desirable. Therefore, the one-pot procedure for the synthesis of $C_{14}N_2H_9SeCl$ in ME media was attempted which involves low reaction time and avoids the use of toxic solvents as compared to conventional methods for synthesis of organochalcogen compounds.[44−49] We hereby report the first ever organoselenide synthesis in ME media.

Being microheterogeneous, microemulsions are excellent solvents for both lipophilic organic substances and polar reagents, such as inorganic and organic salts. Performing the reaction in a microemulsion is therefore a useful way to overcome the solubility problems that are frequently encountered in organic synthesis. This can be attributed to the large interfacial area and high dynamics of MEs.[51] Many organic compounds have a polar and a nonpolar end. Such molecules will orient at the oil−water interface.[52−54] Attack by a water-soluble species will then preferentially occur from the water side and vice versa for water insoluble reagents. Since $C_4N_2H_2Cl_2$ is insoluble in water and isooctane, the reaction is expected to take place at the interface. The oil−water interface[55] and the selected

SCHEME 3: Probable Mechanism for the Synthesis of 4-Chloro-2-(naphthalen-2-ylselanyl) Pyrimidine

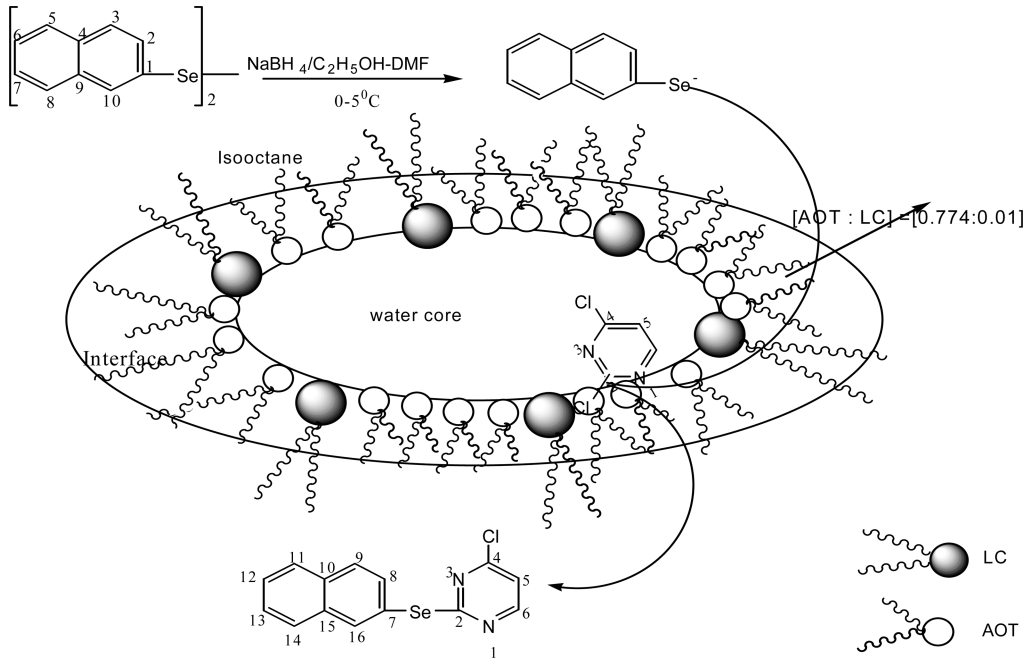

stoichiometric amounts may induce orientation of reactants in microemulsion system, which might lead to selective nucleophilic substitution of chlorine atom at second position of pyrimidine. The reaction proceeds with the reduction of Nap_2Se_2 with $NaBH_4$ to yield $NapSe^-$ anion. The $C_4N_2H_2Cl_2$ is expected to stay at the interface where the electron cloud of the surfactant interface interacts with the electric field produced by the $NapSe^-$. The local hydrobhobicity of the napthyl ring drags the $NapSe^-$ to the interface. The synthesis of $C_{14}N_2H_9SeCl$ in ME media involves nucleophilic substitution reaction of chloride ion at C-2 carbon of $C_4N_2H_2Cl_2$ by $NapSe^-$ anion. The possible mechanism of the reaction has been proposed in Scheme 3.

The synthesis of $C_{14}N_2H_9SeCl$ has been confirmed by the combination of spectroscopic studies viz., ^{1}H NMR, ^{13}C NMR, ^{77}Se NMR, mass spectra, and FT IR. Figure 1 (supporting material) show the representative, ^{1}H NMR, ^{77}Se NMR and mass spectra of the $C_{14}N_2H_9SeCl$.

The obtained product reveals presence of aromatic protons with: δ 8.39−8.35 (d, J 8.1, 1H), δ 8.16−8.12 (m, 2H), δ 8.04−7.98 (m, 2H), δ 7.63−7.59 (m,3H), δ 6.52−6.50 (d, J 5.2, 1H). On the other hand the proton spectra of Nap_2Se_2 shows 7.90−7.98 (d, 2H), 7.45−7.50 (t, 6H), 7.08−7.22 (m, 4H), 6.91−6.96 (t, 2H). The more electron withdrawing effect of pyrimidyl ring in case of $C_{14}N_2H_9SeCl$ accounts for the downfield shift.

In comparison to ^{1}H NMR, the chemical shift values in ^{13}C NMR are more sensitive and lie over a broad range of about ∼240 ppm. Thus, this technique constitutes an important tool for the characterization of organoselenium compounds. The ^{13}C NMR spectra of $C_{14}N_2H_9SeCl$ shows the presence of following peaks, δ 175.09, 160.63, 157.24, 137.41, 134.56, 134.45, 131.88, 128.97, 128.11, 127.67, 126.25, 124.29, 118.73. The spectrum reveals the presence of naphthyl and pyrimidine rings in the studied compound. The C-2 of the pyrimidine ring is highly deshielded due to the two nitrogen and the selenium atom and appears at the highest δ value, i.e., 175.09, followed by the C-4 of pyrimidine ring attached to electron withdrawing chlorine atom with δ value at 160.63. The δ values at 157.24 and 137.41 correspond to C-5 and C-6, respectively. The carbons of the naphthyl ring have chemical shift positions at δ 134.56(C-7), 134.45(C-15), 131.88(C-16), 128.97(C-8), 128.11(C-14), 127.67(C-10), 126.25(C-11), 124.29(C-12, C-9), 118.73 (C-13). This confirms the presence of napthyl and pyrimidyl ring in the compound.

^{77}Se NMR has proved to be a potential method for the characterization of Se compounds. The electron cloud surrounding Se is three times as large as a proton, making its nucleus sensitive even to small changes in the chemical environment. Therefore, evaluation of the ^{77}Se NMR gives a significant insight into the distribution of electron density around selenium metal center.[56] Resonance occurs at δ 429.70 ppm in the case of Nap_2Se_2, whereas it shifts to δ 427.57 ppm in case of $C_{14}N_2H_9SeCl$, unsymmetrical selenium compound, confirming the attachment of single Se in the obtained product.

The isotopic richness of natural Se helps in the identification of Se containing fragments in the mass spectrum of organoselenium compounds. The mass spectra of several diselenides have been reported in literature.[20,57] For the prepared selenide, the molecular ion peak is absent probably due to the high energy associated with electron beam in the electron impact mode. In the obtained spectra the prominent fragment ion peak appears for $[C_{14}N_2H_9Se]^{+\bullet}$ and $[C_{14}N_2H_9SeCl]^{+\bullet}$ +3 at 285 and 323, respectively. FT IR spectra of the obtained product further confirm the formation of $C_{14}N_2H_9SeCl$. The region from 1300−1600 cm^{-1} show clear peaks at 1541.5 and 1399.1 cm^{-1}. This has been presented in Figure 4. The peaks at 1541.5 and 1399.1 cm^{-1} are due to C═C of pyrimidine moiety. For the region 500−800 cm^{-1}, the peaks at 665.4 and 791.0 cm^{-1} have been assigned to C−Se and C−Cl bonds of the obtained product.

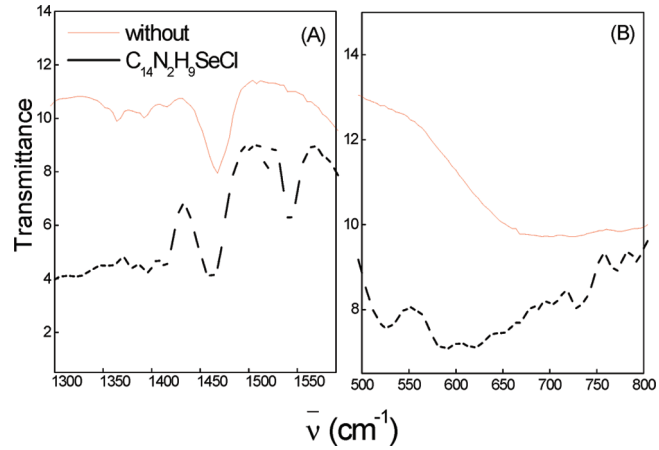

Figure 4. Representative FTIR spectra of $C_{14}N_2H_9SeCl$ in various regions (A) 1200−1700 amd (B) 500−800 cm^{-1}.

Knowledge of the mixed surfactant systems could have many applications in material synthesis. The expanded range of micellar geometries and functionalities available in mixed surfactant systems not only makes them useful for applications but also provides opportunities for fundamental studies of self-assembly. Surfactant solutions are of significant interest in synthesis of nanostructures and synthetic compounds.[56,57] The surfactant combinations described here fall in the category of systems in which aqueous phase synthesis may be combined with organic phase synthesis to create new tools for synthetic chemistry. The obtained knowledge of physiochemical parameters provides an easy route for variation of the structural parameters needed for such research efforts. The ability to selectively modify the microstructure through composition or temperature change also benefit in directing the morphological synthesis of materials.

Conclusions

The incorporation of organodiselenides in microemulsion significantly affects the solubilization and electric percolation phenomenon. ME-II serves as a better host for the assimilation of organodiselenides as compared to ME-I. The better behavior of ME-II further provides a gateway for synthesis of $C_{14}N_2H_9SeCl$. Conductivity and spectroscopy results indicate the presence of ionic interactions between organodiselenides, AOT, and water molecules. The probing of water pool and interfacial properties reveals that organodiselenide molecules are restricted at the interface in ME-II. This understanding of physical parameters and interactions has implications for the design of surfactant systems for organic synthesis. This finds a way for the first ever attempt for synthesis of $C_{14}N_2H_9SeCl$ in ME-II media. The synthetic procedure for the synthesis of $C_{14}N_2H_9SeCl$ reported hitherto is simple, convenient and does not involve troublesome manipulations and use of toxic solvents.

Acknowledgment. S.K.M. and K.K.B. are grateful to DST and CSIR for financial assistance. K.K. and E.A. are thankful to CSIR for fellowships.

Supporting Information Available: ^{1}H NMR, ^{77}Se NMR, and mass spectra of 4-chloro-2-(naphthalen-2-ylselanyl) pyri-

midine ($C_{14}N_2H_9SeCl$) and experimental details of thermodynamics of droplet clustering. This material is available free of charge via the Internet at http://pubs.acs.org.

References and Notes

(1) Eicke, H. F. *Top. Curr. Chem.* **1980**, *87*, 85–145.
(2) Schubel, D.; Ilgenfritz, G. *Langmuir* **1997**, *13*, 4246–4250.
(3) Papadimitriou, V.; Xenakis, A.; Lianos, P. *Langmuir* **1993**, *9*, 912–915.
(4) Papoutsi, D.; Lianos, P.; Brown, W. *Langmuir* **1993**, *9*, 663–668.
(5) Schelly, Z. A. *Curr. Opin. Colloid Interface Sci.* **1997**, *2*, 34–92.
(6) Pant, D.; Riter, R. E.; Levinger, N. E. *J. Chem. Phys.* **1998**, *109*, 9995–10003.
(7) Cho, C. H.; Chung, M.; Lee, J.; Nguyen, T.; Singh, S.; Vedamuthu, M.; Yao, S.; Zhu, J. B.; Robinson, G. W. *J. Phys. Chem.* **1995**, *99*, 7806–7812.
(8) Garcıa-Rıo, L.; Herves, P.; Mejuto, J. C.; Perez-Juste, J.; Rodrıguez-Dafonte, P. *Langmuir* **2000**, *16*, 9716–9721.
(9) Riter, R. E.; Undiks, E. P.; Kimmel, J. R.; Levinger, N. E. *J. Phys. Chem. B* **1998**, *102*, 7931–7938.
(10) Liveri, M. L. T.; Liveri, V. T. *J. Colloid Interface Sci.* **1995**, *176*, 101–104.
(11) Hait, S. K.; Moulik, S. P.; Rodgers, M. P.; Burke, S. E.; Palepu, R. *J Phys. Chem. B* **2001**, *105*, 7145–7154.
(12) Garcia-Rio, L.; Mejuto, J. C.; Perez-Lorenzo, M.; Rodriguez-Alvarez, A.; Dafonte, P. R. *Langmuir* **2005**, *21*, 6259–6264.
(13) Meier, W. *Langmuir* **1996**, *12*, 1188–1192.
(14) Paul, B. K.; Mitra, R. K. *Colloids Surf. A* **2006**, *273*, 129–140.
(15) De, T. K.; Maitra, A. *Adv. Colloid Interface Sci.* **1995**, *59*, 95–193.
(16) Schurtenberger, P.; Magid, L. J.; King, S. M.; Linder, P. *J. Phys. Chem.* **1991**, *95*, 4173–4176.
(17) Wabel, C. Ph.D. Dissertation, University of Erlangen, 1998.
(18) Simmons, B.; Agarwal, V.; McPherson, G.; John, V.; Bose, A. *Langmuir* **2002**, *18*, 8345.
(19) Simmons, B. A.; Irvin, G. C.; Agarwal, V.; Bose, A.; John, V. T.; McPherson, G. L.; Balsara, N. P. *Langmuir* **2002**, *18*, 624–632.
(20) Bhasin, K. K.; Neelam; Rajeev; Gupta, D.; Mehta, S. K.; Klapoetke, T. M.; Crawford, M.-J. *J. Organomet. Chem.* **2004**, *689*, 3327–3334.
(21) Hori, T.; Sharpless, K. B. *J. Org. Chem.* **1979**, *44*, 4208–4210.
(22) Zhang, H.; Daves, G. *J. Org. Chem.* **1993**, *58*, 2557–2560.
(23) Runowicz, C. D.; Fields, A. L.; Goldberg, G. L. *Cancer* **1995**, *76*, 2028–2041.
(24) Gardener, C. R. *General Pharmacology* **1995**, *26*, 245–271.
(25) Ghosh, K. K.; Pandey, A.; Roy, S. *J. Phys. Org. Chem.* **1999**, *12*, 493–498.
(26) Ghosh, K. K.; Roy, S. *Bull. Chem. Soc. Jpn.* **1996**, *69*, 3417–3422.
(27) Berndt, D. C.; Sendelbach, L. E. *J. Org. Chem.* **1977**, *42*, 3305–3306.
(28) Bunton, C. A.; Gillitt, N. D.; Mhala, M. M.; Moffatt, J. R.; Yatsimirsky, A. K. *Langmuir* **2000**, *16*, 8595–8603.
(29) Fernandez, E.; Garcia-Rio, L.; Dafonte, P. R. *J. Phys. Chem.* **2007**, *111*, 11437–11442.
(30) Hager, M.; Currie, F.; Holmberg, K. *Organic Reactions in Microemulsions* **2003**, *227*, 53–74.
(31) Hong, D.-P.; Kuboi, R.; Komasawa, I. *Korean J. Chem. Eng* **1997**, *14*, 334–340.
(32) Fontanella, M. E.; Pieruccini, M.; Salvato, G.; Trusso, S.; Vasi, C.; Lechner, R. E. *Colloid Polym. Sci.* **2002**, *280*, 193–202.
(33) Aliotta, F.; Fazio, B. *Physica A: Statistical Mechanics and its Applications* **2002**, *304*, 111–118.
(34) Hait, S. K.; Moulik, S. P.; Palepu, R. *Langmuir* **2002**, *18*, 2471–2476.
(35) Maitra, A.; Mathew, C.; Varshney, M. *J. Phys. Chem.* **1990**, *94*, 5290–5292.
(36) Li, S.; Irvin, G. C.; Simmons, B.; Rachakonda, S.; Ramannair, P.; Banarjee, S.; John, V. T.; Mc Pherson, G. L.; Zhou, W.; Bose, A. *Colloids Surf. A* **2000**, *174*, 275–281.
(37) Caponetti, E.; Martino, D. C.; Ferrante, F.; Pedone, L.; Ruggirello, A.; Liveri, V. T. *Langmuir* **2003**, *19*, 4913–4922.
(38) Ceglie, A.; Colafemmina, G.; Monica, M. D.; Palazzo, G. *Colloids Surf. A* **1993**, *72*, 285–293.
(39) Zhou, N.; Li, Q.; Wu, J.; Chen, J.; Weng, S.; Xu, G. *Langmuir* **2001**, *17*, 4505–4509.
(40) Garcia-Rio, L.; Godoy, A.; Dafonte, P. R. *Eur. J. Org. Chem.* **2006**, *15*, 3364–3369.
(41) Bergson, G.; Cleson, G.; Schotte, L. *Acta Chem. Scand.* **1962**, *16*, 1159–1174.
(42) Gasco, A.; Dimodica, G.; Barni, E. *Ann. Chim. Rome* **1968**, *58*, 385–396.
(43) Campbell, T. W.; Walker, H. G.; Coppinger, G. M. *Chem. Rev.* **1952**, *50*, 279–283.
(44) Sandhu, A.; Singh, S.; Bhasin, K. K.; Verma, R. D. *J. Fluorine Chem.* **1990**, *47*, 249–259.
(45) Tani, H.; Inamasu, T.; Suzuki, H. *Heterocycles* **1992**, *34*, 341–347.
(46) Bhasin, K. K.; Bhandan, B. S.; Singh, J.; Singh, K. N.; Singh, T. *Synth. Commun.* **2002**, *32*, 1319–1325.
(47) Tian, F.; Yu, Z.; Lu, S. *J. Org. Chem.* **2004**, *69*, 4520–4523.
(48) Brewer, M.; Khasnis, D.; Buretea, M.; Berardini, M.; Emge, T. J.; Brennan, J. G. *Inorg. Chem.* **1994**, *33*, 2743–2747.
(49) Nishino, T.; Okada, M.; Kuroki, T.; Watanbe, T.; Nishiyama, Y.; Sonoda, N. *J. Org. Chem.* **2002**, *67*, 8696–8698.
(50) Bhasin, K. K.; Arora, E.; Mehta, S. K. unpublished work.
(51) Holmberg, K. *Curr. Opin. Colloid Interface Sci.* **2003**, *8*, 187–196.
(52) Garcia-Rio, L.; Leis, J. R.; Pena, M. E.; Eglesias, E. *J. Phys. Chem.* **1993**, *97*, 3437–3442.
(53) Lopez, P.; Rodriguez, A.; Munoz, E.; Gomez-Herrera, C.; Sanchez, F.; Moya, M. L. *J. Colloid Interface Sci.* **1994**, *166*, 503–505.
(54) Garcia-Rio, L.; Leis, J. R.; Eglesias, E. *J. Phys. Chem.* **1995**, *99*, 12318–12326.
(55) Garti, N.; Holmberg, K. *Curr. Opin. Colloid Interface Sci.* **2003**, *8*, 135–136.
(56) Lardon, M. *J. Am. Chem. Soc.* **1970**, *92*, 3005–3009.
(57) Oddershede, J.; Henricksen, L.; Larson, S. *Org. Biomol. Chem.* **2003**, *1*, 1053–1060.

JP902801G